THE JOURNAL OF PHYSICAL CHEMISTRY C
A JOURNAL OF THE AMERICAN CHEMICAL SOCIETY

pubs.acs.org/JPCC
Article

Elucidating the Synergistic Effects of Temperature Rise Inhibitor at the Water Tricalcium Silicate Interface

Jiale Huang, Xabier M. Aretxabaleta, Yu Yan, Zhangli Hu,* Hegoi Manzano,* and Jiaping Liu

Cite This: J. Phys. Chem. C 2024, 128, 6800−6812
Read Online

ACCESS | Metrics & More | Article Recommendations | Supporting Information

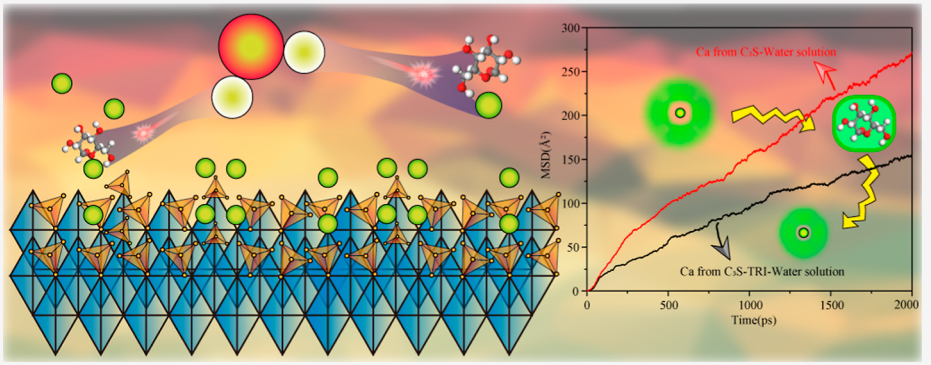

ABSTRACT: Organic−inorganic composites play a crucial role in modulating concrete properties, encompassing interfacial interactions and their synergistic mechanisms. Unraveling these interactions presents a formidable challenge. In this study, molecular dynamics simulations were employed to probe the intricate structure, competition, and equilibrium state of interfacial connections involving a temperature rise inhibitor (TRI), C_3S, and water. Computational results reveal that the interplay of different bonding networks significantly influences the equilibrium state of the C_3S−TRI interfacial interactions, marked by dynamic adsorption−desorption equilibria. The interaction between C_3S and TRI manifests in intricate calcium−oxygen and hydrogen bonding networks, which are both easily disturbed by water molecules. Oxygen sites in water serve as binding sites for calcium atoms in C_3S and hydrogen atoms in TRI, thereby attenuating the C_3S−TRI bonding. Simultaneously, hydrogen sites in water engage with oxygen sites in the TRI, diminishing calcium−oxygen bonding and prompting the detachment of TRI from the C_3S surface. Moreover, these hydrogen sites interact with the oxygen sites on the C_3S surface, inducing lattice structure alterations and removal of calcium atoms from C_3S. As TRI detaches into the liquid phase, it forms complexes with calcium ions, reducing the migration rate of calcium ions within the liquid phase. This study represents the inaugural comprehensive evaluation of the interfacial interaction mechanism between TRI, C_3S, and water, offering fundamental insights into the impact of TRI on the evolution of the C_3S phase. These findings contribute to a deeper understanding of the complex interplay governing concrete properties, paving the way for enhanced control and optimization in concrete technology.

1. INTRODUCTION

In recent years, sustainable buildings have emerged as a pivotal endeavor in cutting CO_2 emissions, significantly shaping urbanization dynamics.[1−3] These sustainability initiatives encompass diverse strategies, such as reducing concrete cracking risks,[4] extending the service life of concrete,[5,6] and facilitating carbon capture.[7] Essential within this context, chemical admixtures constitute an important component in civil engineering materials, endowing concrete with enhanced performance, durability, and aesthetic attributes.[8] This intricacy is inherently linked to the interface modulation of concrete components through chemical admixtures. For instance, Mishra et al.[9] delved into the adsorption mechanism of organic agents at the cement interface, quantitatively elucidating aggregation parameters for distinct grinding aids at the tricalcium silicate (C_3S) interface. The interaction of ion transport inhibitors at the capillary interface of hydration products was examined by Huang et al.,[10] employing drug delivery concepts. They subsequently developed a constitutive model involving organic matter to counter salt ion erosion. Zhou et al.[11] enhanced the interfacial bonding of cement composites to increase their tensile and bending resilience. In this context, diverse polymers emerge as viable agents to effect manifold performance enhancements through their interfacial

Received: November 7, 2023
Revised: March 15, 2024
Accepted: March 20, 2024
Published: April 12, 2024

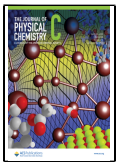

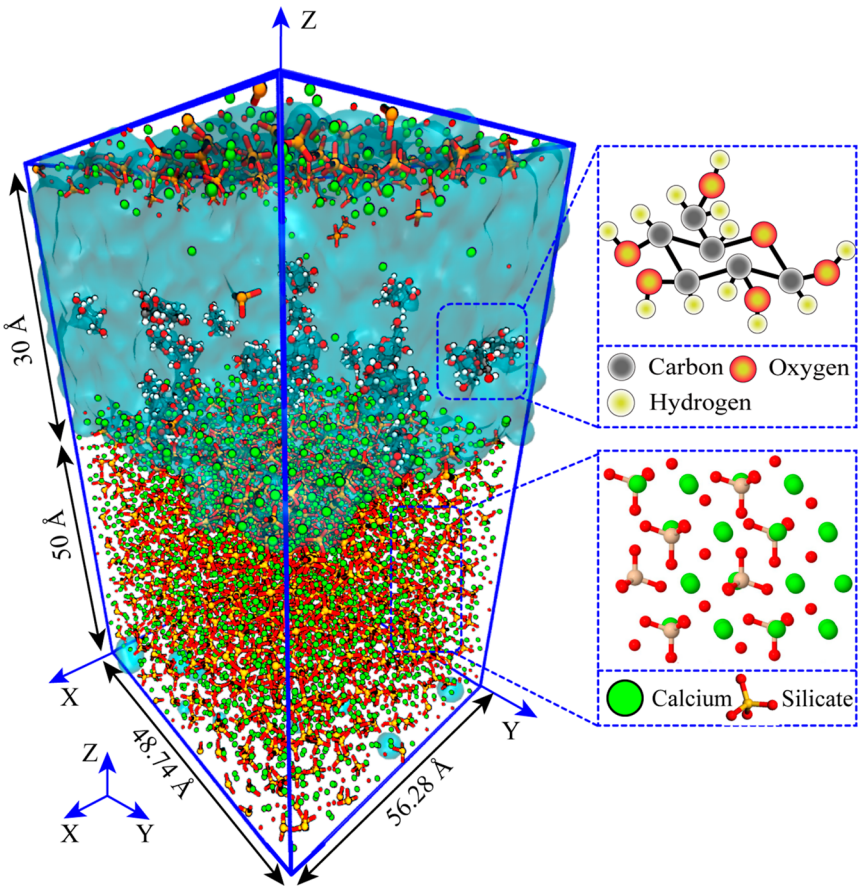

Figure 1. Schematic diagram of the computational model (the lower left side represents the tricalcium silicate region, green balls represent calcium atoms, red and orange balls represent silicate tetrahedra, and the upper left side represents the region of the aqueous solution containing TRI, gray balls represent carbon atoms, red balls represent oxygen atoms, and white balls represent hydrogen atoms. The molecular structure of the TRI monomer is shown in the upper right, and the molecular structure of tricalcium silicate is shown in the lower right).

interactions with phases inherent to cementitious materials.[12−14] Modern buildings are often faced with mass concrete construction, and temperature cracking is the greatest concern in this construction process, which is closely related to the exothermic process of cement hydration.

Given its highest content in cement compositions, C_3S is widely recognized for its pivotal role in governing hydration reactions and the subsequent effects of heat.[15,16] This exothermic heat release rate profoundly influences the equilibrium of internal thermal stress in concrete, thereby influencing the propagation of temperature-induced cracks. Recent studies have introduced a starch-based hydration temperature rise inhibiting material (TRI), grounded in the notion that organic−inorganic composite systems can modulate hydration reactions.[17] At a macroscopic scale, this category of admixture controlled exothermic release during hydration, effectively curbing temperature elevation by reducing the exothermic peak of hydration heat and altering the nature of cement's concentrated exothermic behavior.

Numerous researchers have investigated this fascinating phenomenon. Yan et al.[17,18] proposed that the predominant factor influencing the rise in hydration temperature within cement paste is the conformational evolution of TRI, and this is more important than the effect of degree of polymerization. Additionally, TRI's impact on the initial hydration of C_3S is also attributed to its adsorption on the C_3S surface. Subsequent to TRI depletion, the "second peak" of C_3S hydration occurs, leading to the occurrence of a second exothermic peak. Zhang et al.[19,20] suggested that, on the one hand, the nucleation growth of C−S−H continued only after the continuously generated C−S−H consumed the dissolved TRI, and on the other hand, the dissolved TRI was partially adsorbed on the surface of C−S−H, resulting in the inhibition of C−S−H growth. Although these studies have systematically demonstrated the capacity of TRI to influence the overall hydration process of cementitious materials by exerting an impact on the initial mineral hydration, the microscopic mechanism has not been elucidated due to the limitations of experimental equipment resolution. This phenomenon is intricately linked to the interactions of TRI at the surfaces of cement minerals, particularly C_3S, and the conformational evolution of TRI in solution. Such interactions and their synergistic effects depend on the interfacial interactions among cement minerals, water, and TRI following its incorporation.

To bridge this knowledge gap and gain a deeper understanding of how TRI regulates hydration heat evolution, the mechanisms and synergistic effects between solid and liquid (water and TRI) interfaces are investigated, thereby providing insights at the nanoscale. In this context, molecular dynamics simulations[21−23] can offer reliable insights into the intricate details of the interactions between solid and liquid (water and TRI) interfaces. In this study, the composition, structure, and stability of various interface bonding networks between C_3S and aqueous solutions, with and without TRI, are explained

https://doi.org/10.1021/acs.jpcc.3c07380
J. Phys. Chem. C 2024, 128, 6800−6812

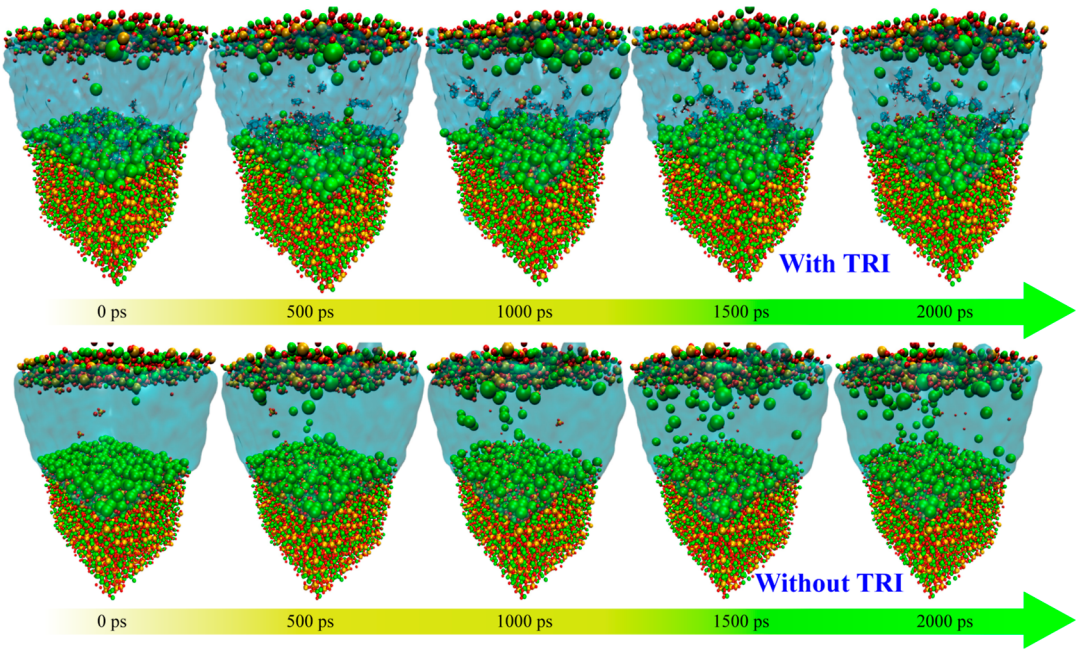

Figure 2. Topological evolution diagram of the tricalcium silicate-water model with and without TRI (upper section depicting interactions in the presence of TRI; green spheres represent calcium atoms, red and orange spheres represent silicate tetrahedra, gray spheres represent carbon atoms, red spheres represent oxygen atoms, and white spheres represent hydrogen atoms; lower section depicts interactions without TRI).

through molecular simulations. This work provides insights into in situ interactions between organic molecules and inorganic minerals at the interfaces.

2. SIMULATION METHODS

The C_3S model employed in this investigation was built based on the crystal structure resolved by NI Golovastikov et al.[24] This structure aligns with the Q-chain distribution of C_3S in cement and X-ray diffraction patterns and has been demonstrated to be suitable for molecular simulations in cement systems.[25] The C_3S-liquid interface model was established, as shown in Figure 1, with dimensions of a = 48.74 Å, b = 56.28 Å, c = 80 Å, $\alpha = 90°$, $\beta = 90°$, and $\gamma = 90°$. A total of 4 × 8 × 2 C_3S unit cells were included. The TRI consisted of a long-chain sugar structure, while a monomer structure was used to investigate the interactions among C_3S, water, and TRI at the interface region. In the solvent region, 20 TRI molecules were randomly placed, and subsequently, water absorption simulation was performed by Monte Carlo, resulting in a liquid-phase water density of 1 g/cm^3.

Subsequently, empirical force fields were employed to examine the interactions between C_3S, water, and the TRI. For C_3S, the CLAYFF force field[26] was utilized, which has been successfully applied to molecular models of clay phases, hydration compounds, and hydroxides. The SPC water model[27] was used to describe the behavior of water and hydroxyl groups. The hydration TRI developed by the Jiangsu Provincial Academy of Building Sciences, has been chosen due to its experimental validation for the suppression of early cement hydration and the mitigation of hydration heat.[17] For the TRI molecules, the consistent valence force field (CVFF)[28] was employed, known for its accurate representation of system structures and binding energies. The CVFF force field is particularly suitable for low-molecular-weight organic crystals and encompasses bond lengths, bond angles, torsional angles, and dihedral interactions. In this study, a hybrid approach was used, where the CLAYFF force field described the interactions between C_3S and water molecules, while the CVFF force field described the TRI molecules.[29] Specifically, both the CLAYFF force field and the CVFF force field use the Lennard-Jones description of van der Waals, with the expression shown in eq 1.

$$E_{\mathrm{VDW}} = \sum_{i \neq j} D_{0,ij}\left[\left(\frac{R_{0,ij}}{r_{ij}}\right)^{12} - 2\left(\frac{R_{0,ij}}{r_{ij}}\right)^{6}\right] \tag{1}$$

The crossed parameters for the organic−inorganic interaction are obtained by the Lorentz−Berthelot mixing rules, with the following expressions shown in equation (eqs 2 and 3)

$$R_{0,ij} = \frac{1}{2}(R_{0,i} + R_{0,j}) \tag{2}$$

$$D_{0,ij} = \sqrt{D_{0,i}D_{0,j}} \tag{3}$$

The LAMMPS software was employed for conducting molecular dynamics simulations.[30,31] For the C_3S dissolution model, an initial energy relaxation was performed using a combination of force fields. Subsequently, a 2 ns dynamics and production process were carried out using the velocity-Verlet integration scheme. During this stage, atomic trajectories were sampled every 0.1 ps for structural and dynamic statistical information. The simulations were carried out under the *NVT* ensemble at 298 K, with a temperature damping parameter of 100 fs and a time step length of 1 fs.

3. RESULTS AND DISCUSSION

The topological configuration, conformational evolution, and interface affinity of TRI with C_3S are reported in Section 3.1. A comparison is drawn with scenarios in which TRI is absent, aimed at investigating the interaction trends of TRI on the

https://doi.org/10.1021/acs.jpcc.3c07380
J. Phys. Chem. C 2024, 128, 6800−6812

surface of C_3S. These observations potentially exhibit their influence on the solid-phase topology and solution environment. The comprehension of intricate interactions between solid and liquid (water and TRI) interfaces is crucial for elucidating the environmental evolution and phenomena occurring when TRI molecules come into contact with cementitious minerals. Subsequent sections, namely, Sections 3.2−3.4, particularly investigate the interactions between each pair of phases. Section 3.5 integrates and discusses the aforementioned subsections. Through the process of dissecting and subsequently reassembling the tripartite interactions, we acquired a more profound understanding of the distinct contributions and synergistic impacts of each phase to the overarching intricate interactions.

3.1. Interaction Tendencies of TRI on the Surface of C_3S. The evolution of the topological configuration of the solid−liquid interface model contributes to the preliminary insights into potential interactions among the respective phases. Figure 2 shows snapshots of the topological changes within C_3S's internal atoms under the presence and absence of TRI. Evidently, as time progresses, the positions of calcium atoms on the surface of C_3S and silicate ions are induced to rearrange due to their interactions with water, transitioning gradually from the solid-phase C_3S to the liquid-phase aqueous solution. This finding aligns with previous results.[21,32,33] To elaborate, in the initial state, the entire system maintains thermodynamic equilibrium, with no repositioning of atoms. As time advances, some calcium atoms exhibit positional changes at 0.5 ns. In the presence of TRI, certain TRI molecules migrate to the solution region, accompanied by conformational rotations, while others adhere to the surface of C_3S. Interestingly, the conformations of TRI adsorbed onto the C_3S surface exhibit variation, with some adopting a perpendicular orientation while others assuming a parallel alignment relative to the C_3S surface. These conformations exhibit a dynamic evolution over time.

Between 1 and 1.5 ns, some calcium atoms migrate to the intermediate region of the liquid phase. When TRI is present, TRI demonstrates a propensity to migrate to the same intermediate region. Figure 2 depicts that the density of calcium atoms in the intermediate region of the liquid phase is noticeably lower in the presence of TRI than in the control group. Additionally, it can be observed that the calcium atoms within the liquid phase region remain in close proximity to TRI, implying a potential interaction between them, which will be studied in Section 3.3. Thus, on the one hand, TRI interacts with the C_3S surface, influencing the interaction between water and the C_3S surface. On the other hand, in the liquid-phase environment, TRI continuously undergoes conformational changes, such as rotations, impacting the distribution density of various atoms within the liquid phase.

For the purpose of analytical clarity, the dynamic evolution of TRI's conformation is consolidated in Figure 3a. Within this depiction, distinctive configurations are denoted: ① signifies TRI's inclination for adsorption onto the C_3S surface, accompanied by ensuing conformational adjustments as portrayed in ②, ③, or ④. Specifically, ② represents stable adhesion onto the C_3S surface, with TRI adopting a flattened orientation. ③ illustrates TRI occupying select vacancies on a segment of the C_3S surface, following the induced restructuring of its topological framework. ④ depicts TRI relinquishing its adhesion from the C_3S surface and transitioning to the solution region due to the intrusion of water. ⑤ represents the entry of

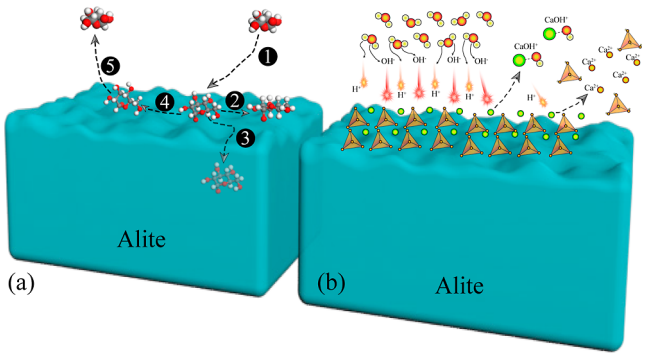

Figure 3. Illustrations of the interactions between TRI and water with tricalcium silicate. (a) Evolutionary diagram depicts the adsorption conformation of TRI on the C_3S surface: gray spheres represent carbon atoms, red spheres represent oxygen atoms, and white spheres represent hydrogen atoms. (b) Topological diagram illustrates the arrangement of water on the C_3S surface: green spheres denote calcium atoms, while red and orange spheres denote silicate tetrahedra.

TRI into the solution region. These intricate processes are closely intertwined with the interactions among TRI, water, and C_3S. This emphasizes the necessity to segregate these interactions into distinct categories, specifically the interactions between C_3S and water, the interactions between C_3S and TRI, and the interactions between TRI and water, prior to amalgamating their individual contributions.

The initial focus is directed toward the interaction between C_3S and water in the absence of TRI. Insights from previous research[21,33] have provided enlightening revelations concerning the interaction between C_3S and water molecules. As depicted in Figure 3b, when water molecules come into contact with C_3S, the dissociation of water molecules leads to the disruption of Si−O−Ca chemical bonds on the surface of C_3S following the well-known proton-metal exchange mechanism.[34,35] When hydrogen ions adhere to the surface of silicate minerals, resulting in the formation of a dissociation layer, the hydroxyl adsorption sites generated through the dissociation of water molecules induce a reduction in the binding between surrounding calcium ions and silicate ions. This effect renders calcium ions more predisposed to form stronger associations with the more reactive hydroxyl groups in water. Subsequently, the mutual binding between silicate ions and calcium ions is further compromised, thereby facilitating the release of ions into the solution. It is worth noting that the force field employed in this study cannot account for the breaking and reforming of bonds. Nonetheless, they effectively characterize interactions between the liquid and solid phases. Thus, the mechanistic section incorporates the aforementioned insights into the explanation, with the aim of unveiling the interactions and synergistic effects between solid and liquid (water and TRI) interfaces. The analysis of the interaction between C_3S and water will be elucidated in detail in Section 3.2.

3.2. Interaction Between C_3S and Aqueous Solution. Subsequently, the focus shifts toward elucidating the interaction between C_3S and TRI. In this context, the interface binding energy is evaluated using LAMMPS to quantitatively characterize the degree of affinity between TRI and the C_3S interface. The temporal profile is presented in Figure 4, indicating that the average adsorption energy between TRI and C_3S remains approximately 300 kcal/mol until the 1.2 ns mark.

https://doi.org/10.1021/acs.jpcc.3c07380
J. Phys. Chem. C 2024, 128, 6800−6812

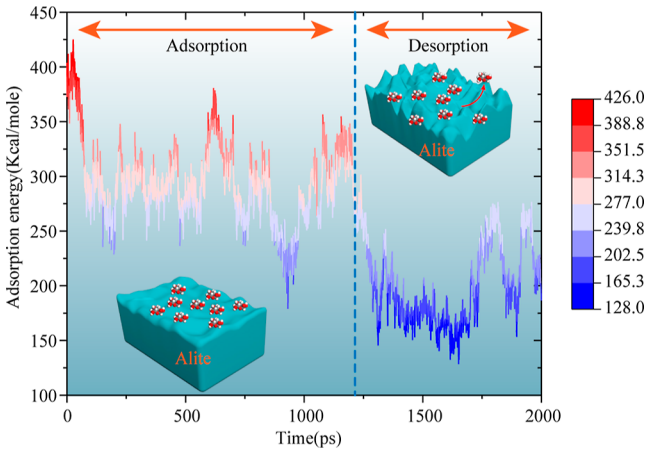

Figure 4. Evolutionary diagram of adsorption and desorption of TRI on the surface of C_3S.

This adsorption behavior corresponds to states ①, ②, and ③, as depicted in Figure 3a. Around the 1.2 ns time frame, a transient fluctuation in the adsorption energy between C_3S and TRI is observed, gradually diminishing over time. The computed average adsorption energy between TRI and C_3S is approximately 175 kcal/mol, aligning with a detachment state represented by conditions ④ and ⑤ in Figure 3a. Importantly, this process showcases a phenomenon of partial adsorption and partial detachment, signifying the existence of diverse interaction modes between C_3S and TRI. Additionally, it suggests a potential competitive adsorption between water and TRI molecules on the C_3S surface. The comprehensive analyses of the interactions involving C_3S and TRI, as well as the interactions between water molecules and TRI, will be expounded in Section 3.3.

The topological evolution of the interface region provides initial insights into the interaction between C_3S and aqueous solutions. Figure 5a,b presents the distribution intensities of calcium and silicate ions at the C_3S interface region, employing the zoning criteria established by Kalinichev.[36] Figure 5a illustrates a gradual decrease in the distribution intensity of calcium ions within the interface region over time, with migration from the interface region to the solution region. Figure 5b shows a similar migration trend for silicate ions as for calcium ions, with a gradually decreasing distribution in the interfacial region and a gradually increasing distribution in the solution region. Part of the dissociated silicate ions still aggregates in the interface region, while a small fraction separates into the solution region.

It is noteworthy that the distribution of calcium ions in the solution region exhibits a trend of aggregation at the interface and boundaries with dispersion in the middle. Taking into consideration the findings from the reports of Manzano et al.,[21] when calcium ions depart from the interface region of C_3S, the original binding sites may be occupied by hydrogen ions in water molecules, yet the charge at these sites remains negative. Consequently, the topological changes in the interface region of C_3S lead to an overall negative charge in this area. However, this negative charge is insufficient to attract calcium ions from the solution region to precipitate onto the C_3S surface due to the presence of hydrogen ions. Furthermore, when water molecules dissociate into hydroxyl groups and hydrogen ions in the solution, part of the hydroxyl groups form hydroxyl-calcium structures by binding to calcium ions that have dissociated from the C_3S surface. At this point, calcium ions on the surface dissolve by changing their coordination from O_{Alite} to O_{Water}.

To characterize this interesting phenomenon, attention is directed toward the coordination numbers (CNs) of calcium ions with oxygen sites on the C_3S surface and hydroxyl sites in water molecules, as illustrated in Figure 6. Changes in the atomic coordination environment can also aid in comprehending the bonding situations of atoms during dynamic processes. Prior to 0.7 ns, the difference in CNs between oxygen in water and calcium ions on the C_3S surface is relatively small, implying competitive adsorption of oxygen in water and oxygen on the C_3S surface for calcium ions. However, as time progresses, after 0.7 ns, the CNs of calcium with oxygen on the C_3S surface gradually decrease, while the CNs of calcium with oxygen in water gradually increase. This indicates that at this point calcium ions detach from the C_3S surface and diffuse outward through oxygen in water molecules. The dissociated hydrogen ions formed by water molecules on the C_3S interface region continually spread into the interior of C_3S, deteriorating the bonding capacity of the C_3S surface. As a result, the bonding interaction ($Ca-O_{C_3S}$) between the C_3S surface and

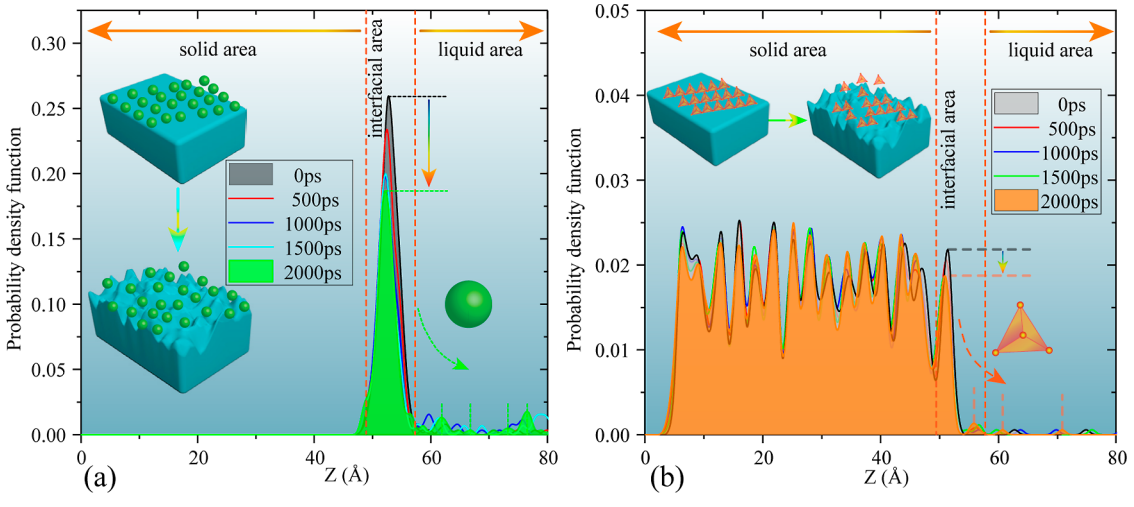

Figure 5. Time-space evolution diagram of ions on the C_3S surface: (a) calcium ions and (b) silicate ions.

https://doi.org/10.1021/acs.jpcc.3c07380
J. Phys. Chem. C 2024, 128, 6800−6812

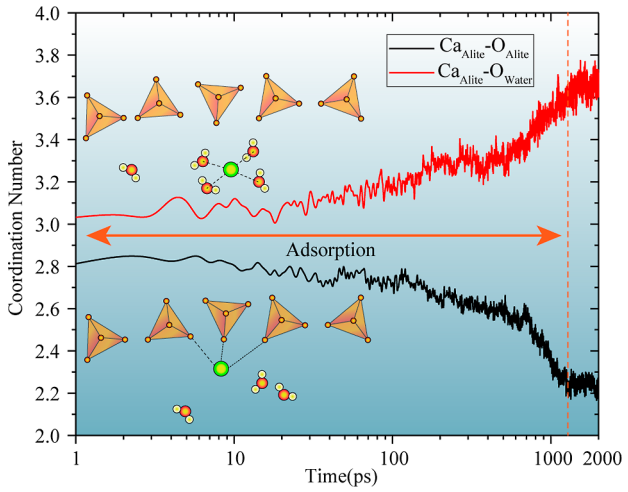

Figure 6. Evolutionary diagram of CNs between calcium atoms in tricalcium silicate and oxygen atoms in water solution, as well as oxygen atoms in tricalcium silicate.

calcium ions is disrupted, leading to the dissolution of calcium ions.

In summary, the atomic topological evolution in the C_3S interface region follows two processes: detachment of atoms from the C_3S surface and diffusion of dissolved ions through the solvent.

3.3. Interaction Between TRI and the C_3S Interface. This section focuses on the interaction between TRI and the C_3S interface region. First, the density distribution function of calcium atoms and silicate ions in the C_3S−water interface region is analyzed and presented in Figure 7a,b. From Figure 7a, it is evident that upon the addition of TRI, the calcium ion distribution in the interfacial region similarly appeared to be reduced. Moreover, in comparison to the situation without TRI, the distribution of calcium atoms in the solution region is more uniform, implying that the presence of TRI might influence the interaction between surface and calcium atoms on the C_3S surface as well as the concentration gradient distribution of calcium atoms in the solution region.

Similarly, it is observed from Figure 7b that the tendency of silicate ions to aggregate in the interface region is relatively weaker compared to the case without TRI. This consistency with the density distribution phenomenon of calcium atoms in the interface area suggests that TRI might influence the attractive forces exerted by the C_3S interface region on the detached ions.

The differences in atomic density distribution are likely triggered by the interaction between TRI and the C_3S interface. The radial distribution function is employed to comprehend the spatial correlations of atoms, offering extensive insights into the interaction between TRI and C_3S. As depicted in Figure 8a, the spatial correlations of calcium atoms on the C_3S surface are examined. Calcium atoms can interact with silicate tetrahedra on the C_3S surface, water molecules, and oxygen sites in TRI to form Ca−O bonding networks. The order of interaction probabilities is $Ca_{C_3S}-O_{C_3S}$ > $Ca_{C_3S}-O_{Water}$ > $Ca_{C_3S}-OH_{TRI}$ > $Ca_{C_3S}-O_{TRI}$. Additionally, two oxygen sites in TRI, namely, the hydroxyl oxygen and the oxygen in the carbonyl group, can interact with calcium atoms on the C_3S surface. The structural snapshots in Figure 8b illustrate the various Ca−O bonding interactions, where ② stands for $Ca_{C_3S}-O_{C_3S}$ that represents the internal bonding within C_3S, with a peak value at around 2.3 Å. The interaction distance between $Ca_{C_3S}-O_{Water}$ represented by ① and $Ca_{C_3S}-O_{TRI}$ represented by ③ and ④ is 2.4 and 2.6 Å, respectively. Notably, TRI contains two types of oxygen sites that can interact with calcium ions in C_3S: the hydroxyl oxygen site represented by ③ and the oxygen site in the carbonyl group represented by ④. The results from the radial distribution function indicate a more probable interaction between calcium atoms and hydroxyl oxygen atoms. This is attributed to the hydroxyl oxygen atoms being more capable of providing lone pair electrons than the oxygen atoms in the carbonyl group, in addition to having smaller spatial hindrance. The shorter interaction distance between calcium atoms and water molecules compared to that between calcium atoms and TRI can be attributed to the smaller volume of polar water molecules, which allows them to approach calcium atoms more easily. This observation is consistent with the findings of Lu et al.'s study on the binding characteristics of sugars and calcium ions based on FTIR spectroscopy.[37]

Furthermore, Figure 9 illustrates that the hydrogen sites of TRI can also form hydrogen bonding networks with oxygen atoms of silicate groups at the C_3S interface with a bonding

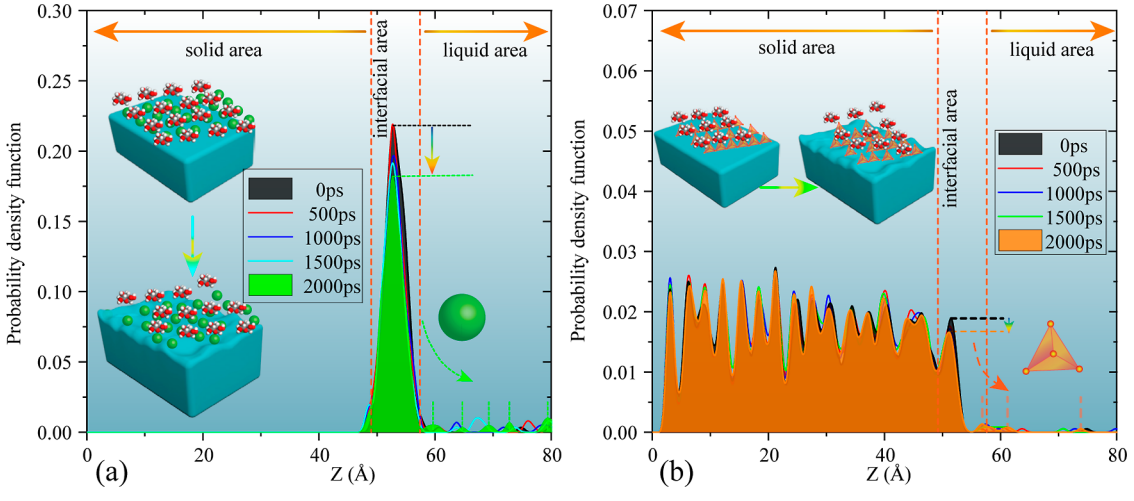

Figure 7. Space-time evolution of ion density distribution on the surface layer of C_3S with TRI: (a) calcium ions and (b) silicate ions.

https://doi.org/10.1021/acs.jpcc.3c07380
J. Phys. Chem. C 2024, 128, 6800−6812

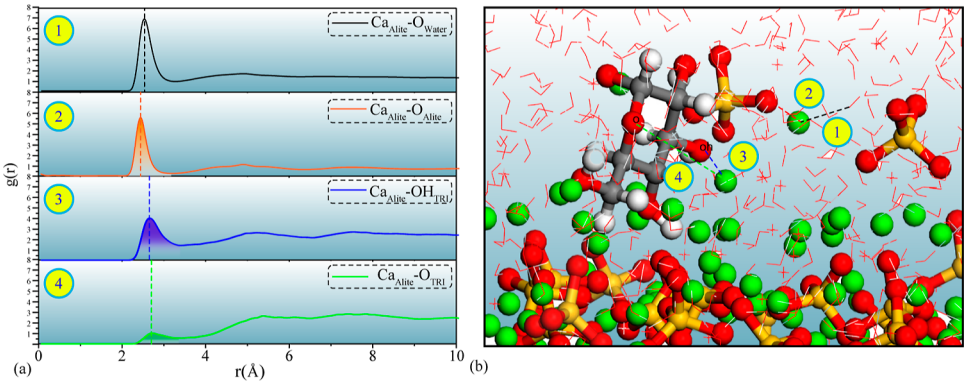

Figure 8. Radial distribution functions of calcium atoms in C_3S with respect to oxygen atoms in different phases (green spheres represent calcium atoms, red and orange spheres represent silicate tetrahedra, gray spheres represent carbon atoms, red spheres represent oxygen atoms, and white spheres represent hydrogen atoms).

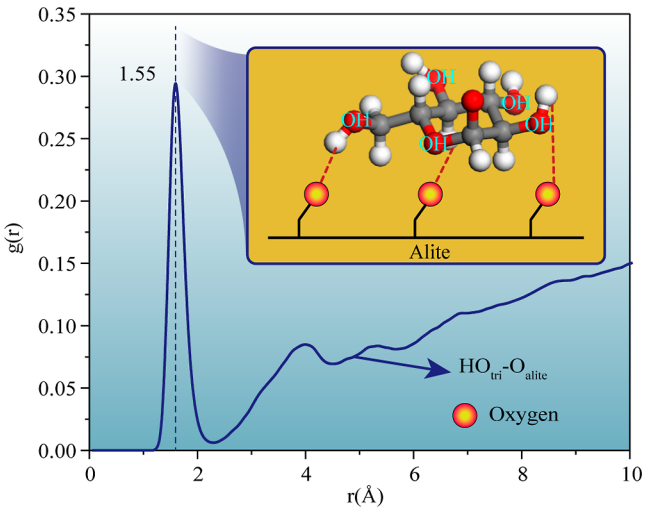

Figure 9. Radial distribution function graph of oxygen atoms in C_3S interacting with hydrogen atoms in TRI.

distance of approximately 1.55 Å. This implies that the interaction between TRI and the C_3S surface is not solely based on a Ca−O bonding network; there is also a presence of hydrogen bonding networks. However, previous studies[10,38] have shown that hydrogen bonding networks are less stable compared to Ca−O bonding networks and are susceptible to disruption by water molecules. Considering the analysis presented earlier, we propose that the adsorption and desorption of TRI on the C_3S surface likely result from the dynamic evolution of TRI−C_3S interactions influenced by water molecule disturbances. This dynamic evolution contributes to the synergistic effects between solid and liquid (water and TRI) interfaces at the interface region. A more detailed analysis is provided in Section 3.5, following the elucidation of the mechanisms and evaluation of the stability of various bonding networks involved in TRI−water molecule interactions.

Thereafter, it can be observed that the calcium atoms on the C_3S surface are intricately involved in a complex network of interactions with oxygen atoms in C_3S, oxygen atoms in water molecules, and oxygen atoms in TRI. These interactions form a competitive environment for various Ca−O bonding interactions, influencing the physicochemical state of calcium atoms, such as their charge, chemical interactions, hydration effects, and solubility. Ultimately, this competition could impact the evolution of the C_3S surface's topological structure. Therefore, the coordination environment of calcium atoms on the C_3S surface is investigated to uncover this intricate competition.

Figure 10 illustrates the changes in the coordination environment of calcium atoms in a TRI solution. The CN of

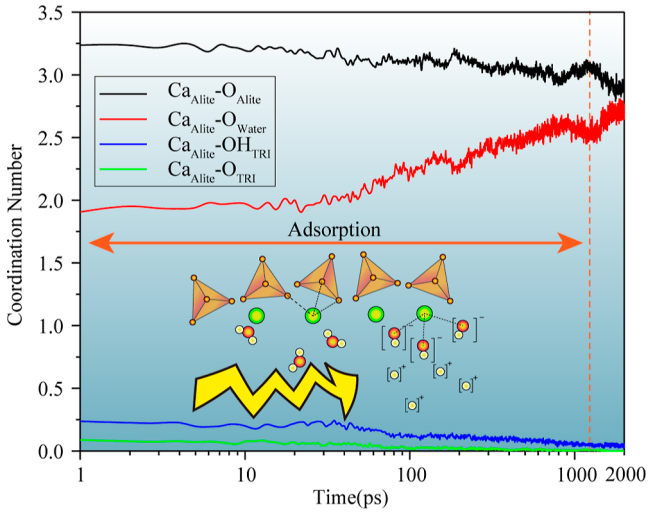

Figure 10. Evolution of CNs of calcium atoms in C_3S with respect to oxygen atoms from water solution, calcium silicate, and TRI.

calcium atoms with oxygen in water gradually increases over time, while the CN with oxygen in C_3S decreases. As mentioned earlier, this suggests that calcium atoms at the C_3S interface are undergoing dissolution. However, in the presence of TRI, the CN of calcium atoms with oxygen in water only increases to 2.75 compared to around 3.7 in the water solution. Furthermore, the CN of calcium atoms with oxygen in C_3S decreases to 2.75, while it decreases to around 2.2 in the water solution. This further indicates that the interaction between calcium atoms on the C_3S surface and oxygen atoms in water molecules is restricted in the presence of TRI interference. This observation supports the mechanism of interaction between TRI and C_3S discussed in the previous section. Some calcium atoms break their bonds with C_3S due to the influence of TRI, but they are partially retained on the C_3S surface due to the binding effect of TRI molecules.

https://doi.org/10.1021/acs.jpcc.3c07380
J. Phys. Chem. C 2024, 128, 6800−6812

Beyond the interaction observed between a fraction of TRI molecules adhering to the surface of C_3S and calcium atoms, there is an additional interaction occurring between a subset of TRI molecules and the liberated calcium atoms within the solution. In the aqueous environment, the diffusion kinetics of atoms play a pivotal role in governing cementitious chemical reactions, encompassing equilibrium phenomena such as dissolution−precipitation equilibrium and the nucleation and growth processes of calcium−silicate−hydrate (C−S−H) phases. In this context, the mean square displacement function emerges as an invaluable tool, furnishing comprehensive insights into the dynamic behavior of atoms within the liquid phase. A comprehensive record of the mean square displacement functions corresponding to calcium atoms within diverse solution environments is meticulously presented in Figure 11.

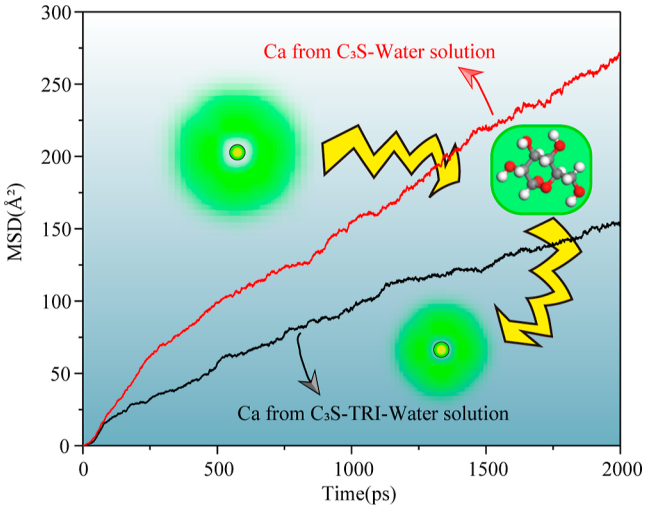

Figure 11. Mean square displacement function of calcium atoms in tricalcium silicate solution systems with and without TRI.

Globally, the diffusion propensity of calcium atoms within the TRI solution environment exhibits conspicuous attenuation compared to their behavior in an aqueous solution, as informed by the kinetic dynamics of TRI−C_3S interactions. This tempered diffusion trend of calcium atoms within the TRI environment can be ascribed to a dual influence. Primarily, preceding the 0.1 ns interval, a complete congruence of the mean square displacement functions of calcium atoms is evident in both solution contexts. Nevertheless, as TRI progressively engages with the C_3S interface, effectuating intricate networks of calcium−oxygen bonds and hydrogen bonds, the topographical architecture of the C_3S surface undergoes a fortification process due to the transformative actions of TRI. Consequently, the mobility of calcium atoms on the C_3S surface becomes restricted, as they become entrapped by the augmenting TRI−C_3S interplay. Over time, this dynamic interaction is perturbed by the ingress of water molecules, prompting a diversified structural evolution of TRI. This evolution encompasses scenarios wherein TRI adheres to the C_3S surface and alternately remains unbound within the solution medium.

Concurrently, at the juncture of 1.2 ns, Figure 4 showcases a discernible trend toward TRI detachment. Furthermore, discernible in Figure 11, a subtle inflection point characterizes the diffusion profile of calcium atoms within the TRI solution. This pivotal juncture signifies a reduction in the slope of the mean square displacement function, indicating that despite the precipitation of calcium atoms into the solution environment, free TRI molecules within the solution retain their propensity to engage in bonding interactions with these calcium atoms. Consequently, this phenomenon induces a gradual decrease in the diffusion capacity of calcium atoms. In summation, it is evident that TRI exerts a multifaceted influence—by orchestrating interactions with the C_3S surface, TRI impacts the topological evolution of the C_3S interface, and by engaging with calcium atoms emancipated into the solution milieu, TRI regulates the migration velocity of calcium atoms.

3.4. Interaction Between TRI and Aqueous Solution.

TRI demonstrates a dual capacity: it not only engages with the C_3S surface but also exerts an influence on the migration rate of free calcium ions within the solution. These interactions are primarily contingent upon the conformational changes that TRI undergoes within the solution environment, a phenomenon intrinsically linked to the influence of water molecules. This section is dedicated to exploring the intricate interplay between TRI and water molecules. Initially, the underlying mechanism governing the connection between TRI and water molecules is meticulously examined, leading to the identification of pivotal functional groups. Subsequently, by leveraging the insights gleaned from the preceding analysis, coupled with the evolving distribution and transformation of functional groups, a comprehensive elucidation of the intricate interaction dynamics between water molecules and TRI is presented.

Figure 12 depicts the radial distribution functions that elucidate the intricate interactions between water molecules

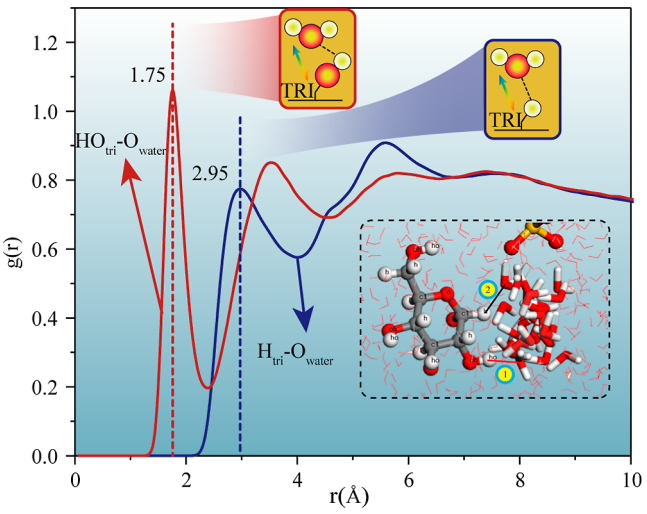

Figure 12. Radial distribution function depicting the interaction between TRI and water molecules.

and the distinct hydrogen bonding sites on TRI. As shown in Figure 12, pronounced hydrogen bonding occurrences are observed between the oxygen atoms within water and both the hydroxyl and carbon−hydrogen sites on TRI. However, a noteworthy disparity arises in the extent of these hydrogen bonding interactions. Specifically, the first peak of the RDF associated with TRI's hydroxyl hydrogen sites is positioned around 1.75 Å, whereas for the carbon−hydrogen sites, it is situated at approximately 2.95 Å. This distinct contrast highlights the hydroxyl hydrogen sites as the primary sites of binding engagement. Concomitantly, the hydroxyl sites serve

https://doi.org/10.1021/acs.jpcc.3c07380
J. Phys. Chem. C 2024, 128, 6800−6812

as binding sites for the interaction between TRI and calcium ions within both TRI and C_3S. Hence, the dynamic binding behavior at these specific sites potentially has a decisive influence over the intricate calcium ion interactions.

The spatiotemporal evolution of the density distribution of functional groups within TRI, specifically hydroxyl groups, was systematically analyzed and is presented in Figure 13.

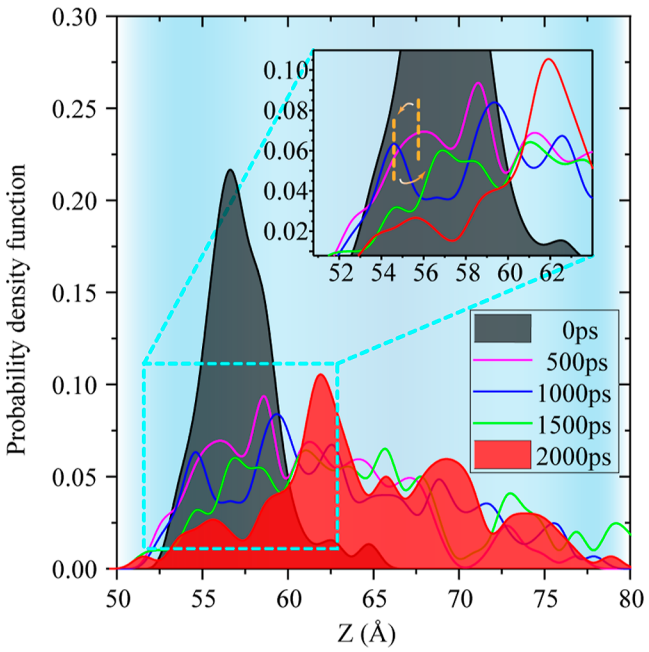

Figure 13. Time-varying density distribution of hydroxyl functional groups in TRI in the solution region.

Observations derived from the figure illustrate distinctive trends: the hydroxyl functional groups on TRI molecules exhibit a leftward shift in their first peak at 0.5 ns compared to the initial state, followed by another leftward shift at 1 ns, and subsequently a gradual rightward shift after 1.5 ns. This evolution corresponds to the appearance of partial diffusion of TRI molecules, which coincides with the commencement of the phenomena detailed in Section 3.1. This validation further confirms the sequential adsorption and subsequent desorption of TRI molecules from the C_3S surface. The underlying rationale for this phenomenon can be attributed to the intricate bonding interactions established between the calcium atoms at the C_3S interface and TRI molecules. However, these bonding interactions are susceptible to the perturbing influence of water molecules. Specifically, hydroxyl oxygen sites within TRI and calcium within C_3S can form bonds, albeit with a lower probability than bonds between calcium and internal oxygen in C_3S or oxygen in water. This disparity suggests interference in the connection between TRI and calcium on the C_3S surface, rendering TRI unable to achieve stable adsorption on the C_3S surface through calcium−oxygen bonding.

Furthermore, Figure 9 visually represents the formation of hydrogen bonding interactions between TRI's hydrogen sites and C_3S's oxygen sites, although with a relatively modest binding strength. Inspection of TRI's inherent molecular configuration reveals a pervasive distribution of hydrogen sites across the carbon ring. The formation of hydrogen bonding networks significantly influences TRI's conformation on the C_3S surface. Specifically, the greater the number of hydrogen sites binding on the carbon ring, the tighter the association between TRI and C_3S, resulting in a propensity for TRI to lie more horizontally on the C_3S surface. Concurrently, the structural integrity of the C_3S surface is enhanced. On one hand, water molecules, owing to TRI's spatial hindrance effect, face challenges in interacting with the reinforced C_3S surface. On the other hand, water molecules necessitate the disruption of the hydrogen bonding network formed between TRI and C_3S before they can dissociate from the C_3S surface. This undoubtedly amplifies the demand for the dissolution driving forces. These two distinct modes of bonding interaction collectively account for the phenomenon of partial detachment and partial adsorption of TRI at the interface. This correlation aligns with the TRI−C_3S interaction elucidated in Section 3.3.

3.5. Synergistic Mechanism of the Interaction Network among C_3S, Water, and TRI. The preceding sections have separately dissected the interactions involving C_3S and water, C_3S and TRI, and TRI and water. This detailed analysis has furnished a wealth of information that is pivotal for unraveling the synergistic mechanisms governing the interactions between solid and liquid (water and TRI) interfaces within the interfacial region. This section aims at consolidating the three interactions mentioned above, evaluating the stability of all bonding networks, and proposing a collaborative mechanism for the C_3S−water−TRI interaction network based on the earlier delineated mechanisms.

The accuracy of the adsorption properties of TRI on the surface of C_3S, as well as the complexation with calcium ions in solution, as proposed by molecular dynamics, was experimentally verified. For this purpose, a TOC (MultiN/C 3100) was utilized to test the adsorption properties of TRI in cement as well as in C_3S, and ion chromatography (IC, Dionex DP series ICS-3000) was employed to measure the concentration of calcium ions in the pore solution. In Figure S1, it can be observed that TRI can be adsorbed in both C_3S and cement systems. However, the amount of adsorption in the cement system is significantly stronger than that in the C_3S system. This suggests that, on the one hand, the adsorption capacity of the rest of the mineral phases in the cement system with TRI is stronger than that of the C_3S with TRI, and, on the other hand, TRI is not completely adsorbed on the surface of the C_3S, as mentioned in the previous conclusions. As mentioned previously, some TRI adsorbs on the surface of C_3S, and some TRI will be free in the solution system. Both types of interactions are influenced by water molecules. Figure S2 shows that the concentration of calcium ions detected in the pore solution after the addition of TRI was slightly lower than that of the control group. Interestingly, after 12 h, the concentration of calcium ions in the experimental group with the addition of TRI was higher than that in the control group, and the difference in the calcium ion concentration between the two experimental groups first increased and then decreased. This suggests that initially, TRI forms complexes with calcium ions, causing a decrease in the concentration of free calcium ions in the pore solution, and as the reaction proceeds, this complexation is disrupted by water molecules.

The stability of bonding interactions is intricately linked to the strength and dynamic characteristics of the interactions. To assess the stability of such bonding interactions, time correlation functions (TCFs) are employed, as depicted by the equation (eq 4).

https://doi.org/10.1021/acs.jpcc.3c07380
J. Phys. Chem. C 2024, 128, 6800−6812

$$\mathrm{TCF} = \frac{\langle \delta b_s \delta b_0 \rangle}{\langle \delta b_0 \delta b_0 \rangle} \quad (4)$$

where $\delta b_s = b_s - \langle b \rangle$, and b_s is a binary operator. If a connection is established, the TCF value equals 1, and if the connection is destroyed, it becomes 0. $\langle b \rangle$ implies the mean of this operator for all of the pairs and simulation. The definition of connection is based on the information provided by the radial distribution function. Specifically, when the distance between two atoms is smaller than the horizontal coordinate corresponding to the first minima of the radial distribution function, we define it as a connection, and the value of TCF is 1. Conversely, if the distance between two atoms is larger than this horizontal coordinate, it is a nonbonding, and the value of TCF is 0.

Figure 14 depicts the interaction stability between the oxygen sites within each phase (water, TRI, and C_3S) and the

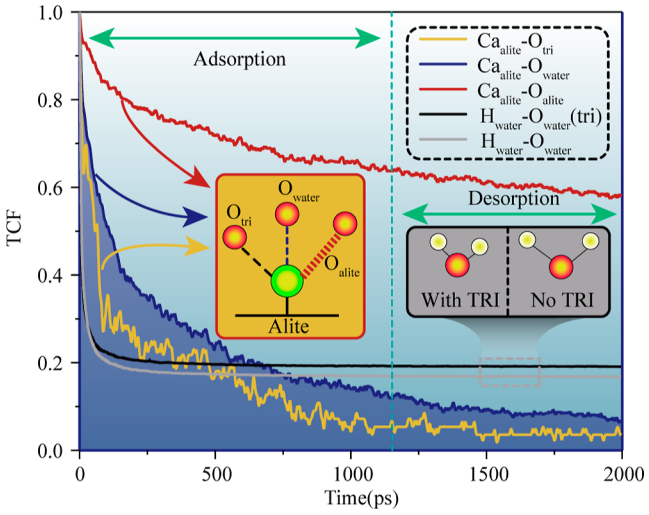

Figure 14. TCF of the C_3S–water–TRI interaction network.

calcium atoms on the C_3S surface in the presence of TRI. Notably, the arrangement of bonding stability among the various bonds is illustrated as

$$Ca_{C3S} - O_{C3S} > Ca_{C3S} - O_{Water} > Ca_{C3S} - O_{TRI}$$

This follows a sequence as that observed in Figure 10, which portrays the order of interaction probabilities of the radial distribution function. The stability of bonding between calcium atoms on the C_3S surface and oxygen atoms exhibits two distinct phases: the adsorption stage spanning 0 to 1.2 ns shown in Figure 4. During this stage, two types of interactions are prevalent between TRI and the calcium atoms on the C_3S surface: calcium–oxygen networks and hydrogen bonding networks, both of which play essential roles in TRI's adsorption. However, water molecules exert a disruptive effect on both of these interactions.

For the calcium–oxygen networks, oxygen sites within water molecules can interact with calcium atoms, and the stability of this interaction is slightly stronger than that of the calcium–oxygen networks formed between TRI and C_3S. Therefore, it can be deduced that a significant portion of the calcium–oxygen networks formed between TRI and C_3S will be disrupted due to the presence of water. As water molecules progressively form a dissociation layer on the C_3S surface, their competition with calcium atoms transitions to the oxygen sites on the C_3S surface. The hydrogen sites within water molecules are responsible for disrupting the interaction between oxygen sites on the C_3S surface and calcium atoms. These hydrogen sites within water molecules bind to oxygen sites on the C_3S surface, weakening the interaction between surface oxygen and calcium atoms. Additionally, hydroxyl sites within water molecules interact with calcium atoms, further diminishing calcium's dependence on the C_3S surface. Consequently, calcium atoms are detached from the C_3S surface, leading to a cascading effect where the interaction between TRI and C_3S is subsequently weakened. At this juncture, TRI gradually migrates into the liquid phase environment.

The stability of bonding between calcium atoms on the C_3S surface and oxygen atoms then transitions to a second stage, occurring after 1.2 ns. During this stage, a fraction of TRI dissociates from the C_3S surface and interacts with calcium atoms that have also detached from the C_3S surface within the liquid-phase environment. It is important to note that at this juncture, calcium atoms interact not only with TRI but also with water molecules. The diffusion of calcium atoms in the liquid phase is directly related to their interactions with both calcium atoms and water molecules. If these interactions are hindered, then the diffusion of calcium atoms is consequently affected. Indeed, it is the interaction between TRI and calcium atoms that results in a reduction in the diffusion rate of calcium atoms in the liquid phase.

It is worth noting that Figure 14 also assesses the bonding stability within water molecules under different solution conditions. However, when TRI is present, the bonding stability within water molecules appears slightly higher

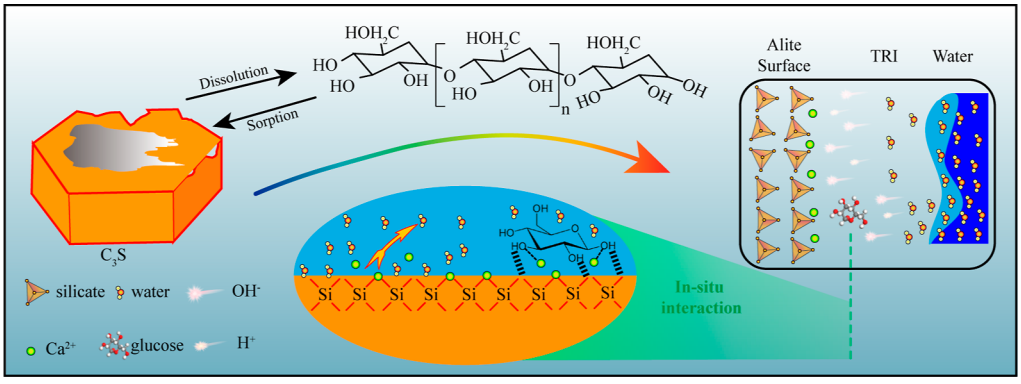

Figure 15. Schematic diagram of the C_3S–water–TRI interaction network.

https://doi.org/10.1021/acs.jpcc.3c07380
J. Phys. Chem. C 2024, 128, 6800–6812

compared to that under conditions without TRI. This phenomenon is intriguing and suggests that the presence of TRI may potentially decrease the dissociation capability of water molecules. As a result, interactions between C_3S and water molecules may not be as pronounced in the presence of TRI compared to situations where TRI is absent. However, this conclusion remains qualitative in nature.

In summary, when TRI is involved in interactions at the C_3S interface, the interactions among different phases influence each other. To investigate the impact mechanism of TRI on C_3S interfacial reactions, it is necessary to decouple these interactions and explore the synergistic effects between them. Figure 15 illustrates a schematic representation of the interactions in the C_3S−water−TRI system. In the presence of TRI, the TRI molecules in the liquid phase environment simultaneously interact with both C_3S and water molecules. When TRI comes into contact with C_3S, the polar functional groups of TRI that interact with C_3S can also disrupt the Si−O−Ca chemical bonds on the C_3S surface. However, unlike water molecules, where dissociated H ions are independently connected to hydroxyl groups, the polar hydroxyl group on the TRI's polar functional group connects with the rest of the hydrogen atoms through covalent bonds, forming a relatively fixed rigid structure.

Therefore, after disrupting the Ca−O−Si bonds, TRI's hydroxyl groups bind with calcium ions, and TRI's hydrogen sites form a hydrogen bond network with oxygen atoms on the silicate group of the C_3S interface. This results in the phenomenon of TRI being adsorbed on the C_3S surface, forming an O_{C_3S}−TRI−Ca_{C_3S} structure. When water molecules come into contact with TRI, the polar functional groups, i.e., hydroxyl groups, attract the hydrogen atoms in water molecules. In other words, TRI undergoes a hydration phenomenon in aqueous solution, which helps in reducing the reactivity of water molecules on the C_3S surface. This implies that water molecules are less likely to form hydrated ions or, if they do, these hydrated ions preferentially adsorb onto TRI. Consequently, this further influences the interfacial interactions between water molecules and C_3S.

4. CONCLUSIONS

This study uses molecular dynamics simulations to investigate the interfacial interaction mechanisms between the solid and liquid (water and TRI) interfaces. By decoupling and recoupling the interaction mechanisms between pairs of these phases, a comparison is made to elucidate the differences in the composition, topology, liquid-phase evolution, and diffusion of the bonding network involved in the C_3S interface reactions with and without TRI.

The interaction dynamics between the TRI and C_3S interfaces exhibits a dual-phase process: adsorption and desorption. Adsorption primarily stems from the calcium−oxygen network between TRI and C_3S, alongside the hydrogen bonding network. These bonding types are easily affected by water molecules, leading to competitive adsorption and subsequent desorption of TRI. This competitive adsorption not only hinders the water interaction with the C_3S surface, specifically impacting the protonation reaction (evidenced by a decrease in the CN of calcium in C_3S and oxygen in the water from 3.7 to 2.75 after doping TRI) but also facilitates TRI's complexation with free calcium ions in the solution upon detachment from the C_3S surface. This, in turn, inhibits the diffusion of calcium ions within the liquid phase, influencing the dissolution−precipitation equilibrium in the hydration reaction and the nucleation growth of C−S−H.

In essence, this study uniquely decouples and recouples the competitive relationships between the solid and liquid (water and TRI) interfaces. The intricate understanding of TRI's role in C_3S dissolution holds significant implications for the design of innovative additives in cement hydration. By shedding light on the complex interplay of these components, this research lays the groundwork for the development of novel strategies to optimize concrete properties, offering potential advancements in cement technology in the future.

■ ASSOCIATED CONTENT

Supporting Information

The Supporting Information is available free of charge at https://pubs.acs.org/doi/10.1021/acs.jpcc.3c07380.

Adsorption diagram of TRI in the C3S system and cement system and calcium ion concentration in pore solution during dissolution of C3S (PDF)

■ AUTHOR INFORMATION

Corresponding Authors

Zhangli Hu − *School of Materials Science and Engineering, Southeast University, Nanjing 211189, China; State Key Laboratory of High Performance Civil Engineering Materials,, Nanjing 211103, China*; Email: zhanglihu@seu.edu.cn

Hegoi Manzano − *Physics Department, Unibersity of the Basque Country UPV/EHU, Leioa 48940 Basque Country, Spain*; orcid.org/0000-0001-7992-2718; Email: hegoi.manzano@ehu.eus

Authors

Jiale Huang − *School of Materials Science and Engineering, Southeast University, Nanjing 211189, China; State Key Laboratory of High Performance Civil Engineering Materials,, Nanjing 211103, China; Physics Department, Unibersity of the Basque Country UPV/EHU, Leioa 48940 Basque Country, Spain*

Xabier M. Aretxabaleta − *Physics Department, Unibersity of the Basque Country UPV/EHU, Leioa 48940 Basque Country, Spain*

Yu Yan − *Department of Civil and Environmental Engineering, National University of Singapore, Singapore 117576, Singapore*

Jiaping Liu − *School of Materials Science and Engineering, Southeast University, Nanjing 211189, China; State Key Laboratory of High Performance Civil Engineering Materials,, Nanjing 211103, China*

Complete contact information is available at: https://pubs.acs.org/10.1021/acs.jpcc.3c07380

Notes

The authors declare no competing financial interest.

■ ACKNOWLEDGMENTS

Authors appreciate the financial support from the Major Program of National Natural Science Foundation of China (grant no. 52293433), the China Scholarship Council (grant no. 202106090091), the "Departamento de Educación, Política Lingüística y Cultura del Gobierno Vasco" (grant no. IT1458-22), and the Transnational Common Laboratory "Aquitaine-

Euskadi Network in Green Concrete and Cement-based Materials" (LTC-Green Concrete). We are also grateful to the High-Performance Computer Center (HPCC) of Nanjing University and Beijing PARATERA Tech CO., Ltd. for providing HPC resources that have contributed to the research results reported within this paper. During the preparation of this work, J.H. used OPENAI in order to language polishing. After using this tool/service, J.H. reviewed and edited the content as needed and took full responsibility for the content of the publication.

REFERENCES

(1) Martirena, F.; Scrivener, K. Low carbon cement LC3 in cuba: ways to achieve a sustainable growth of cement production in emerging economies. Calcined clays for sustainable concrete. In *Proceedings of the 2nd International Conference on Calcined Clays for Sustainable Concrete*, 2018; pp 318−321.
(2) Schneider, M. The cement industry on the way to a low-carbon future. *Cem. Concr. Res.* **2019**, *124*, 105792.
(3) Mehta, P. K. Greening of the concrete industry for sustainable development. *Concr. Int.* **2002**, *24*, 23−28.
(4) Liu, J.; Tian, Q.; Wang, Y.; Li, H.; Xu, W. Evaluation method and mitigation strategies for shrinkage cracking of modern concrete. *Engineering* **2021**, *7*, 348−357.
(5) Tang, S. W.; Yao, Y.; Andrade, C.; Li, Z. Recent durability studies on concrete structure. *Cem. Concr. Res.* **2015**, *78*, 143−154.
(6) Mehta, P. K. Durability of concrete−fifty years of progress?. In *SP-126: Durability of Concrete: Second International Conference, Montreal, Canada 1991* Special Publication, 1991; Vol. *126*; pp 1−32.
(7) Liu, X.; Feng, P.; Cai, Y.; Yu, X.; Yu, C.; Ran, Q. Carbonation behavior of calcium silicate hydrate (CSH): its potential for CO2 capture. *Chem. Eng. J.* **2022**, *431*, 134243.
(8) Marchon, D.; Flatt, R. *Science and Technology of Concrete Admixtures*; Elsevier, 2016; pp 279−304.
(9) Mishra, R. K.; Flatt, R. J.; Heinz, H. Force field for tricalcium silicate and insight into nanoscale properties: cleavage, initial hydration, and adsorption of organic molecules. *J. Phys. Chem. C* **2013**, *117*, 10417−10432.
(10) Huang, J.; Chen, R.; Zhou, Y.; Ming, J.; Liu, J. Molecular design and experiment of ion transport inhibitors towards concrete sustainability. *Cement Concr. Compos.* **2022**, *133*, 104710.
(11) Zhou, A.; Yu, Z.; Wei, H.; Tam, L.-h.; Liu, T.; Zou, D. Understanding the toughening mechanism of silane coupling agents in the interfacial bonding in steel fiber-reinforced cementitious composites. *ACS Appl. Mater. Interfaces* **2020**, *12*, 44163−44171.
(12) Xie, C.; Niu, Z.; Kim, D.; Li, M.; Yang, P. Surface and interface control in nanoparticle catalysis. *Chem. Rev.* **2020**, *120*, 1184−1249.
(13) Shao, F.; Mi, L.; Tian, Z.; Zheng, C.; Zhang, Y.; Li, Q.; Liu, S. Promoting photodegradation efficiency via a heterojunction photocatalyst combining with oxygen direct and fast diffusion from the gas phase to active catalytic sites. *ACS Appl. Mater. Interfaces* **2019**, *11*, 44922−44930.
(14) Shi, R.; Shang, L.; Zhang, T. Three phase interface engineering for advanced catalytic applications. *ACS Appl. Energy Mater.* **2021**, *4*, 1045−1052.
(15) Scrivener, K.; Ouzia, A.; Juilland, P.; Kunhi Mohamed, A. Advances in understanding cement hydration mechanisms. *Cem. Concr. Res.* **2019**, *124*, 105823.
(16) Scrivener, K. L.; Juilland, P.; Monteiro, P. J. Advances in understanding hydration of Portland cement. *Cem. Concr. Res.* **2015**, *78*, 38−56.
(17) Yan, Y.; Ouzia, A.; Yu, C.; Liu, J.; Scrivener, K. L. Effect of a novel starch-based temperature rise inhibitor on cement hydration and microstructure development. *Cem. Concr. Res.* **2020**, *129*, 105961.
(18) Yan, Y.; Scrivener, K. L.; Yu, C.; Ouzia, A.; Liu, J. Effect of a novel starch-based temperature rise inhibitor on cement hydration and microstructure development: the second peak study. *Cem. Concr. Res.* **2021**, *141*, 106325.
(19) Zhang, H.; Li, L.; Feng, P.; Wang, W.; Tian, Q.; Liu, J. Impact of temperature rising inhibitor on hydration kinetics of cement paste and its mechanism. *Cement Concr. Compos.* **2018**, *93*, 289−300.
(20) Zhang, H.; Wang, W.; Li, Q.; Tian, Q.; Li, L.; Liu, J. A starch-based admixture for reduction of hydration heat in cement composites. *Constr. Build. Mater.* **2018**, *173*, 317−322.
(21) Manzano, H.; Durgun, E.; Lopez-Arbeloa, I.; Grossman, J. C. Insight on tricalcium silicate hydration and dissolution mechanism from molecular simulations. *ACS Appl. Mater. Interfaces* **2015**, *7*, 14726−14733.
(22) Manzano, H.; Moeini, S.; Marinelli, F.; Van Duin, A. C.; Ulm, F.-J.; Pellenq, R. J.-M. Confined water dissociation in microporous defective silicates: mechanism, dipole distribution, and impact on substrate properties. *J. Am. Chem. Soc.* **2012**, *134*, 2208−2215.
(23) Huang, J.; Li, W.; Ma, Y.; Jin, M.; Li, Z.; Manzano, H.; Liu, J. Multiscale deterioration of recycled aggregate gel network via solar irradiation: reaction molecular dynamics and experiments. *J. Clean. Prod.* **2023**, *426*, 139084.
(24) Golovastikov, N. Crystal structure of tricalcium silicate, $3CaOSiO_2 = C_{3S}$. *Sov. Phys. Crystallogr.* **1975**, *20*, 441−445.
(25) Tavakoli, D.; Tarighat, A. Molecular dynamics study on the mechanical properties of Portland cement clinker phases. *Comput. Mater. Sci.* **2016**, *119*, 65−73.
(26) Cygan, R. T.; Liang, J.-J.; Kalinichev, A. G. Molecular models of hydroxide, oxyhydroxide, and clay phases and the development of a general force field. *J. Phys. Chem. B* **2004**, *108*, 1255−1266.
(27) Mark, P.; Nilsson, L. Structure and dynamics of the TIP3P, SPC, and SPC/E water models at 298 K. *J. Phys. Chem. A* **2001**, *105*, 9954−9960.
(28) Dauber-Osguthorpe, P.; Roberts, V. A.; Osguthorpe, D. J.; Wolff, J.; Genest, M.; Hagler, A. T. Structure and energetics of ligand binding to proteins: Escherichia coli dihydrofolate reductase-trimethoprim, a drug-receptor system. *Proteins: Struct., Funct., Bioinf.* **1988**, *4*, 31−47.
(29) Huang, J.; Zhou, Y.; Yang, X.; Dong, Y.; Jin, M.; Liu, J. A multi-scale study of enhancing mechanical property in ultra-high performance concrete by steel-fiber@nano-silica. *Constr. Build. Mater.* **2022**, *342*, 128069.
(30) Plimpton, S.; Crozier, P.; Thompson, A. LAMMPS-large-scale atomic/molecular massively parallel simulator. *Sandia Natl. Lab.* **2007**, *18*, 43.
(31) Thompson, A. P.; Aktulga, H. M.; Berger, R.; Bolintineanu, D. S.; Brown, W. M.; Crozier, P. S.; in 't Veld, P. J.; Kohlmeyer, A.; Moore, S. G.; Nguyen, T. D.; Shan, R.; Stevens, M. J.; Tranchida, J.; Trott, C.; Plimpton, S. J. LAMMPS—a flexible simulation tool for particle-based materials modeling at the atomic, meso, and continuum scales. *Comput. Phys. Commun.* **2022**, *271*, 108171.
(32) Wang, L.; Hou, D.; Shang, H.; Zhao, T. Molecular dynamics study on the Tri-calcium silicate hydration in sodium sulfate solution: interface structure, dynamics and dissolution mechanism. *Constr. Build. Mater.* **2018**, *170*, 402−417.
(33) Qi, C.; Manzano, H.; Spagnoli, D.; Chen, Q.; Fourie, A. Initial hydration process of calcium silicates in Portland cement: a comprehensive comparison from molecular dynamics simulations. *Cem. Concr. Res.* **2021**, *149*, 106576.
(34) Snellings, R. Surface chemistry of calcium aluminosilicate glasses. *J. Am. Ceram. Soc.* **2015**, *98*, 303−314.
(35) Heidmann, I.; Christl, I.; Leu, C.; Kretzschmar, R. Competitive sorption of protons and metal cations onto kaolinite: experiments and modeling. *J. Colloid Interface Sci.* **2005**, *282*, 270−282.
(36) Kalinichev, A. G.; Kirkpatrick, R. J. Molecular dynamics modeling of chloride binding to the surfaces of calcium hydroxide, hydrated calcium aluminate, and calcium silicate phases. *Chem. Mater.* **2002**, *14*, 3539−3549.
(37) Lu, Y.; Deng, G.; Miao, F.; Li, Z. Sugar complexation with calcium ion. Crystal structure and FT-IR study of a hydrated calcium chloride complex of D-ribose. *J. Inorg. Biochem.* **2003**, *96*, 487−492.
(38) Zhou, Y.; Hou, D.; Manzano, H.; Orozco, C. A.; Geng, G.; Monteiro, P. J.; Liu, J. Interfacial connection mechanisms in calcium−

https://doi.org/10.1021/acs.jpcc.3c07380
J. Phys. Chem. C 2024, 128, 6800−6812

silicate−hydrates/polymer nanocomposites: a molecular dynamics study. *ACS Appl. Mater. Interfaces* **2017**, *9*, 41014−41025.

https://doi.org/10.1021/acs.jpcc.3c07380
J. Phys. Chem. C 2024, 128, 6800−6812